

Performance of Propellers

The performance of a propeller is typically presented using the following characteristics

$$F = \text{Propeller Thrust} \quad ; \quad T = \text{Propeller Torque} \quad ; \quad v_{mi1} = \text{Inflow velocity far upstream} \quad (\text{Mfc1})$$

and the following non-dimensional parameters; the advance ratio J_1 , the flow coefficient, J_p , the thrust coefficient, C_F , the torque coefficient, C_T , and the efficiency, η (see section (Mfd)), defined as follows:

$$J_1 = \frac{\pi v_{mi1}}{R\Omega} \quad ; \quad J_p = \pi\phi = \frac{\pi v_{mp1}}{R\Omega} \quad ; \quad C_F = \frac{F}{\rho R^2 \Omega^2 A_p} \quad (\text{Mfc2})$$

$$C_T = \frac{2T}{\rho R^2 \Omega^2 A_p} \quad ; \quad \eta = \frac{F v_{mi1}}{\Omega T} \quad (\text{Mfc3})$$

where R and Ω are the propeller radius and radian frequency of rotation, the flow notation is defined below and ϕ is the flow coefficient used in describing pump flows.

In what follows we present an approximate, one-dimensional analysis of the performance of a propeller mounted in a wind or water tunnel since that is typically the context in which performance measurements are made. The influence of the tunnel walls will emerge from the performance data presented.

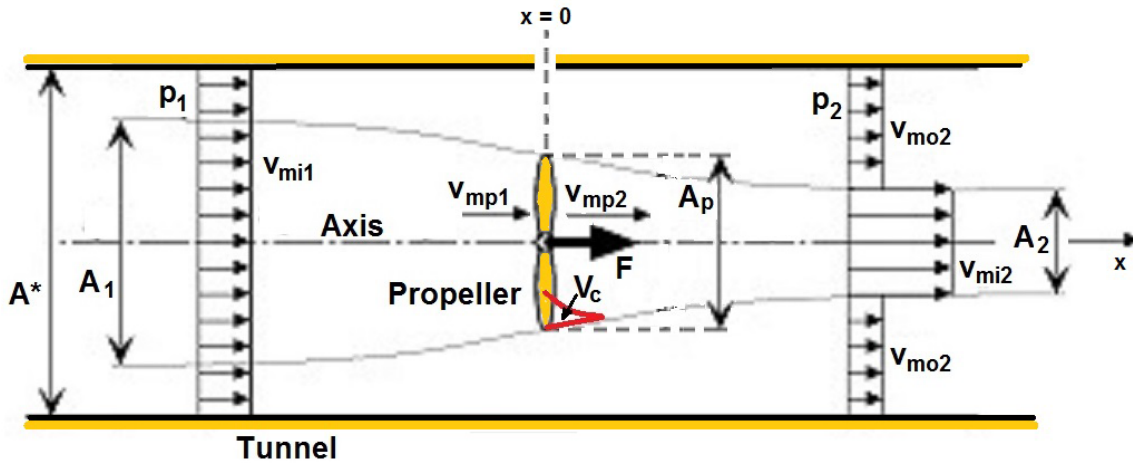


Figure 1: Schematic and notation of a propeller in a tunnel; the cavitation volume is shown in red.

Consider the one-dimensional, incompressible flow through a propeller (either cavitating or non-cavitating) in a wind or water tunnel as shown in Figure 1. The propeller (cross-sectional area A_p) is located on the centerline of the tunnel whose cross-sectional area is A^* . We consider both the stream tube that proceeds through the propeller and the external stream tube that does not pass through the propeller. For simplicity, it will be assumed that the flow is uniformly distributed across these stream tubes and is one-dimensional. Friction and mixing losses between the inner and outer stream tubes are neglected. Mass conservation in this steady flow requires that

$$v_{mi1}A_1 = v_{mp1}A_p = v_{mi2}A_2 \quad ; \quad v_{mp2} = v_{mp1} \quad ; \quad v_{mi2}A_2 + v_{mo2}(A^* - A_2) - v_{mi1}A^* = 0 \quad (\text{Mfc4})$$

where v_{mi} and v_{mo} denote velocities in the inner and outer flows, A denotes the cross-sectional area of the inner stream tube, and the additional subscripts 1, 2 and p respectively denote quantities far upstream (or

at the propeller inlet), far downstream (or at the propeller discharge), and at the propeller itself. It has been assumed that the velocities in inner the outer flows are the same far upstream. The relation between the pressures far upstream and far downstream is obtained by applying Bernoulli's equation in the outer flow as follows:

$$p_2 - p_1 = \frac{1}{2}\rho \{v_{mi1}^2 - v_{mo2}^2\} \quad (\text{Mfc5})$$

The thrust force F produced by the propeller may be assessed using three relations. First, the momentum theorem applied to a control volume containing all the tunnel flow yields;

$$F = \frac{1}{2}\rho(v_{mi1} - v_{mo2})A^*(2v_{mi2} + v_{mo2} - v_{mi1}) \quad (\text{Mfc6})$$

Second, the total pressure difference across the propeller, Δp^T , follows from the Euler head as

$$\Delta p^T = \rho R\Omega(R\Omega - v_{mp2} \cot \beta) \quad (\text{Mfc7})$$

where β denotes the discharge flow angle from the blades. Since the static pressure difference, $p_{p2} - p_{p1}$, is given by

$$p_{p2} - p_{p1} = \frac{1}{2}\rho \{R^2\Omega^2 - v_{mp2}^2 \cot^2 \beta\} \quad (\text{Mfc8})$$

the thrust force can be computed as

$$F = \frac{1}{2}\rho \{R^2\Omega^2 - v_{mp2}^2 \cot^2 \beta\} A_p \quad (\text{Mfc9})$$

Third, the pressures p_{p1} and p_{p2} may be related to the upstream and downstream conditions using Bernoulli's equation:

$$p_{p1} = p_1 + \frac{1}{2}\rho v_{mi1}^2 - \frac{1}{2}\rho v_{mp1}^2 \quad (\text{Mfc10})$$

Applying Bernoulli's equation between the outlet of the propeller and far downstream, we obtain

$$\begin{aligned} p_{p2} &= p_2 + \frac{1}{2}\rho [v_{mi2}^2 + v_{\theta p2}^2 (A_p/A_2)] - \frac{1}{2}\rho [v_{mp2}^2 + v_{\theta p2}^2] \\ &= p_2 + \frac{1}{2}\rho v_{mi2}^2 - \frac{1}{2}\rho v_{mp2}^2 + \frac{1}{2}\rho [R\Omega - v_{mp2} \cot \beta]^2 [(A_p/A_2) - 1] \end{aligned} \quad (\text{Mfc11})$$

Then the thrust force F follows as

$$F = (p_{p2} - p_{p1})A_p = \frac{1}{2}\rho [\{v_{mi2}^2 - v_{mo2}^2\} + \{R\Omega - v_{mp2} \cot \beta\}^2 \{(A_p/A_2) - 1\}] A_p \quad (\text{Mfc12})$$

The total mass flow rate and static pressure downstream of the propeller are defined downstream of the mixing of the flows in the inner and outer stream tubes. The mass flow rate and pressure after mixing, m_2 and p'_2 , are obtained by applying continuity and momentum conservation as follows:

$$m_2 = \rho [v_{mi2}A_2 + v_{mo2}(A^* - A_2)] = \rho v'_{mi2}A^* \quad (\text{Mfc13})$$

$$p_2A^* + \rho v_{mi2}^2A_2 + \rho v_{mo2}^2(A^* - A_2) = p'_2A^* + \rho v_{mi2}'^2A^* \quad (\text{Mfc14})$$

Summarizing, we note that the eight equations (Mfc4) through (Mfc12) contain eight unknowns v_{mo2} , v_{mi2} , v_{mp2} , v_{mp1} , A_1 , A_2 , F , and p_2 assuming that the propeller operating parameters v_{mi1} , p_1 , $R\Omega$, and the discharge flow angle, β , are given. For present purposes the discharge flow angle, β , is assumed known and independent of the other flow parameters except when cavitation occurs; this case is examined in the

section on cavitation performance. With this in mind, we will proceed to discuss the steady flow solutions of equations (Mfc4) to (Mfc12). These equations can be solved provided the operating conditions, v_{mi1} , p_1 , $R\Omega$ and the discharge flow angle, β , are specified. For the purposes of illustration, we choose to present results for a typical discharge flow angle of $\beta = 25^\circ$. The results are presented using the non-dimensional parameters; the advance ratio J_1 , the propeller flow coefficient J_p and the propeller thrust coefficient, C_T .

Note that as the incoming velocity, v_{mi1} , is decreased, the inner stream tube expands far upstream and its cross-sectional area, A_1 , reaches that of the tunnel, A^* , at a certain value of v_{mi1} . When the incoming velocity is smaller than this value, equation (Mfc5) no longer applies. In such cases, the steady solution is obtained by setting $A_1 = A^*$ and $v_{mo2} = 0$, and eliminating the last of equations (Mfc4), because it becomes identical to the combination of the first three.

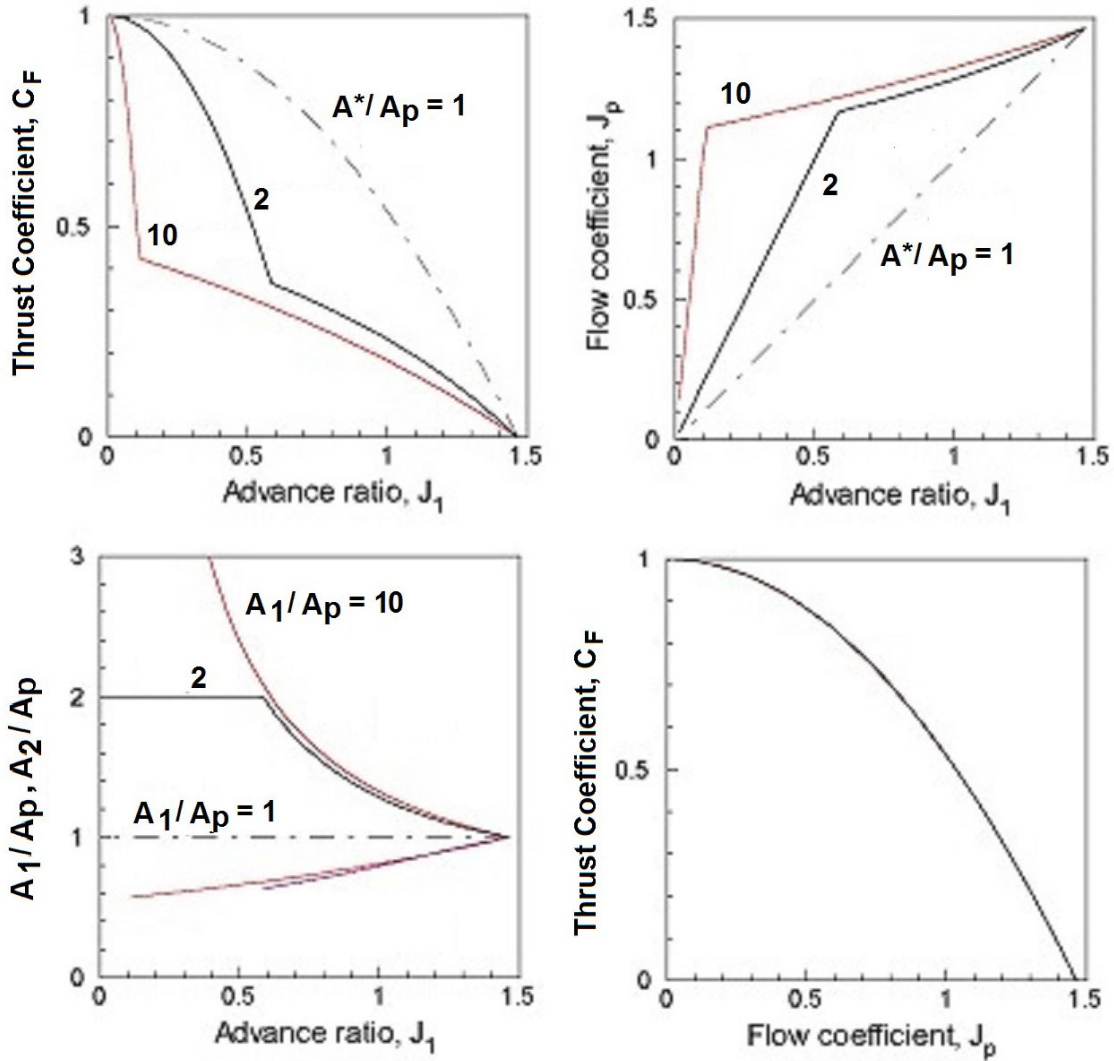


Figure 2: Steady characteristics of a non-cavitating propeller with a discharge flow angle of $\beta = 25^\circ$. The propeller is located at the center of the duct with cross-sectional areas of $A^*/A_p = 1, 2$ and 10 .

Typical results are shown in Figure 2. Various values of the cross-sectional area ratio, A^*/A_p , were selected in order to examine the effect of the presence of the tunnel walls. The case with $A^*/A_p = 1$ corresponds closely to that of a typical axial flow pump, because all the flow from upstream proceeds through the propeller (assuming no tip leakage flow for simplicity) and there is no outer flow. For the cases with

$A^*/A_p = 2$ and 10, a *critical advance ratio*, J_1^* (approximately $J_1^* = 0.58$ and 0.12 for $A^*/A_p = 2$ and 10, respectively) exists at which the cross-sectional area of stream tube far upstream, A_1 , is equal to that of the duct, A^* . Below the critical advance ratio, the propeller works like a axial flow pump with all the fluid flowing through the propeller. The results for $A^*/A_p = 10$ have been found to adequately represent the open condition ($A^*/A_p = \infty$) except at very low advance ratios, where the analysis breaks down for reasons discussed elsewhere.

Figure 2 presents the thrust coefficient, C_F , the propeller flow coefficient, J_p , and the cross-sectional areas, A_1/A_p and A_2/A_p , plotted against the advance ratio, J_1 . For $A^*/A_p = 2$ and 10, as the advance ratio decreases, the flow coefficient decreases gradually and the thrust coefficient increases gradually. This is because, as the advance ratio is decreased, the propeller is taking fluid from a wider upstream stream tube. The variations of the thrust coefficient and the flow coefficient are more gradual than those for $A^*/A_p = 1$. However, below the critical advance ratio where the propeller works like an axial flow pump, the flow coefficient rapidly decreases and the thrust coefficient rapidly increases, and these variations are more significant than for $A^*/A_p = 1$. The decrease in the flow coefficient is related directly to the advance ratio, so that the slope of the flow coefficient in Figure 2 gets steeper as the duct gets wider.